Electronic Supplementary Material (ESI) for Catalysis Science & Technology.
This journal is © The Royal Society of Chemistry 2018

Supplementary Information

Micropore blocked core-shell ZSM-22 designed via epitaxial growth with enhanced shape selectivity and high n-dodecane hydroisomerization performance

Pengyu Niu[a,b], Hongjuan Xi[a], Jun Ren[c], Minggui Lin[a], Qiang Wang[a], Xiaoyan Chen[a], Pengfei Wang[a], Litao Jia[a], Bo Hou[a,*], and Debao Li[a,*]

[a] State Key Laboratory of Coal Conversion, Institute of Coal Chemistry, Chinese Academy of Sciences, Taiyuan 030001, People's Republic of China

[b] University of Chinese Academy of Sciences, Beijing 100049, People's Republic of China

[c] School of Chemical and Environmental Engineering, North University of China, Xueyuan Road 3, Taiyuan, 030051, China

* Corresponding Author

E-mail: houbo@sxicc.ac.cn.

dbli@sxicc.ac.cn.

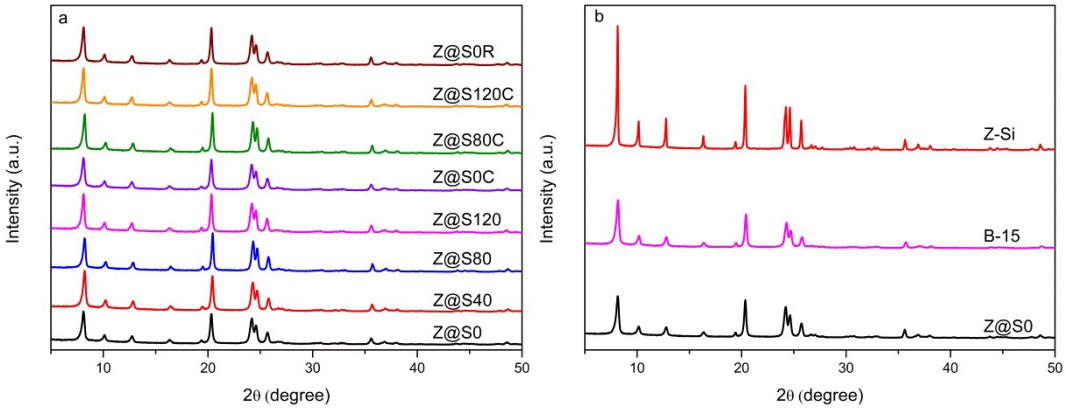

Figure S1. XRD patterns of the studied samples.

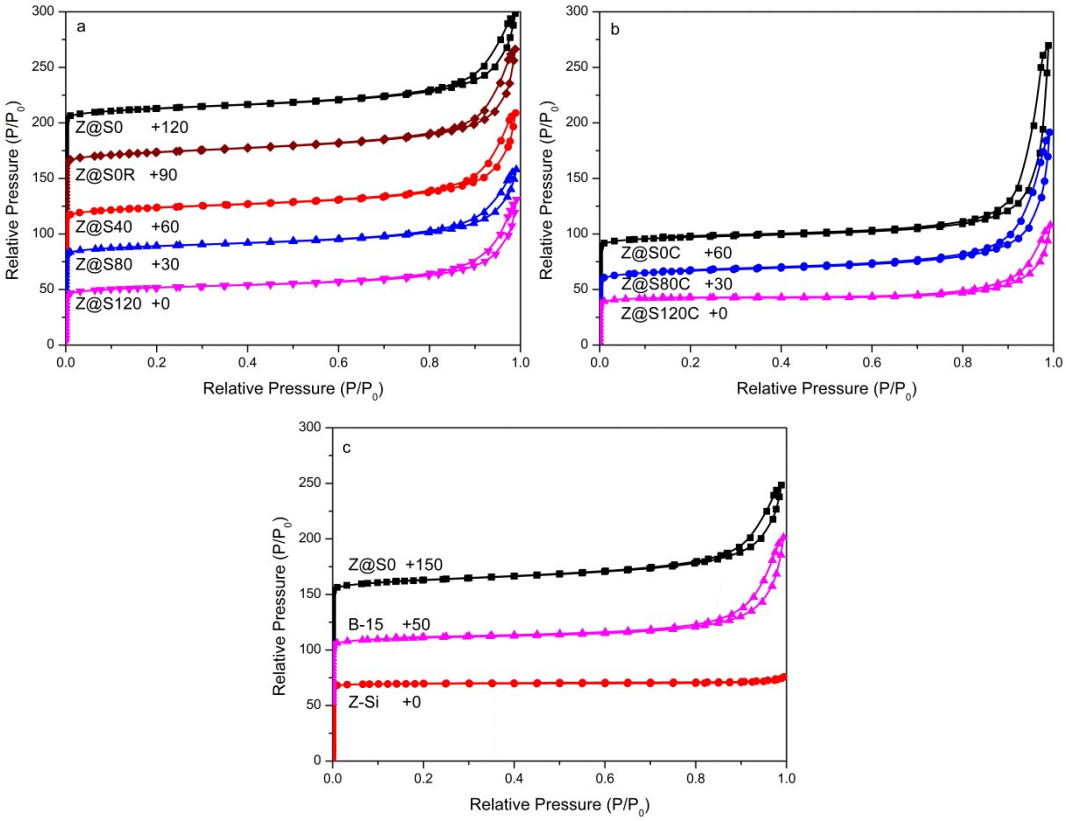

Figure S2. N_2 adsorption and desorption isotherms of the studied samples.

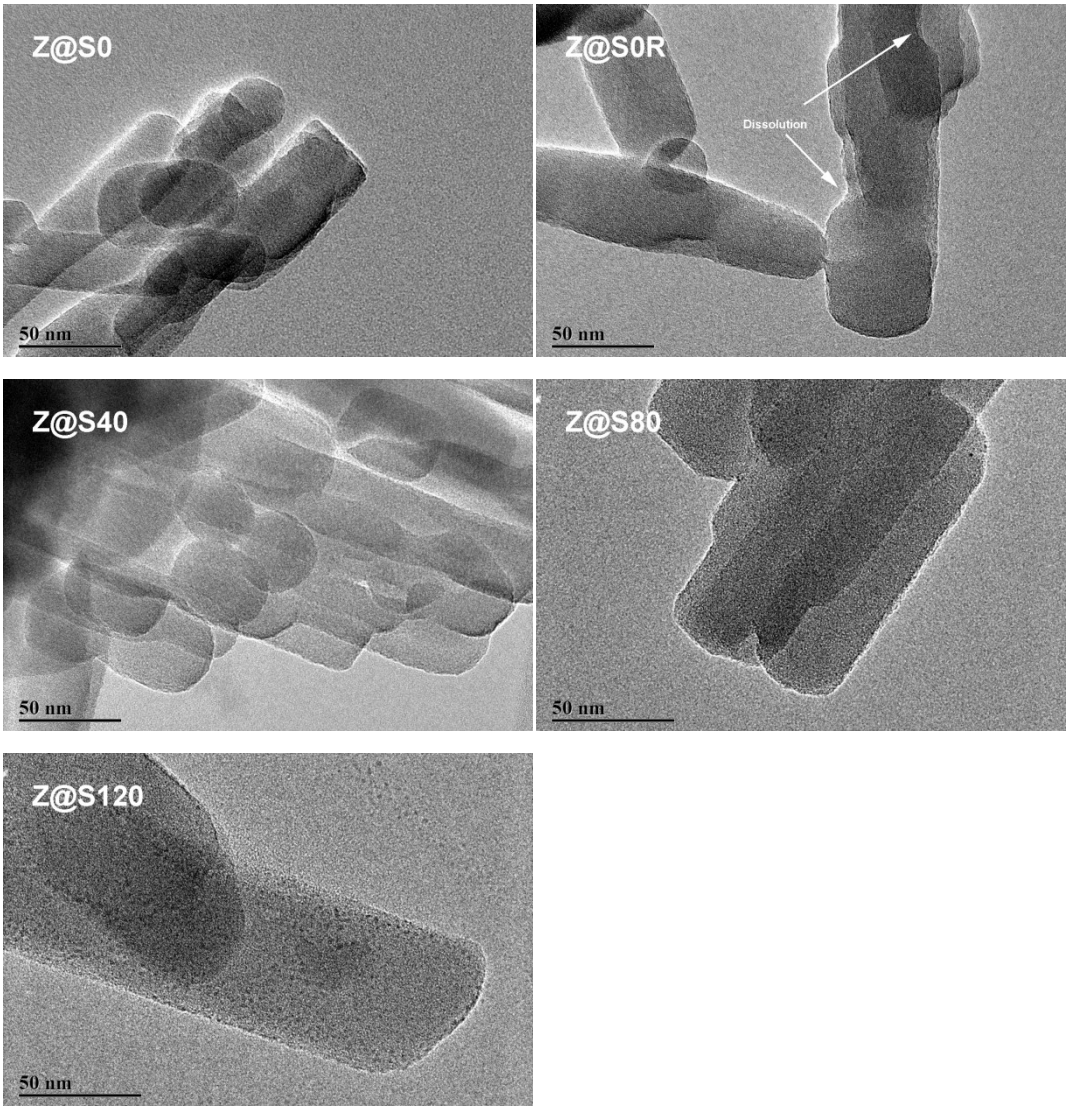

Figure S3. TEM images for ZSM-22@highly siliceous ZSM-22.

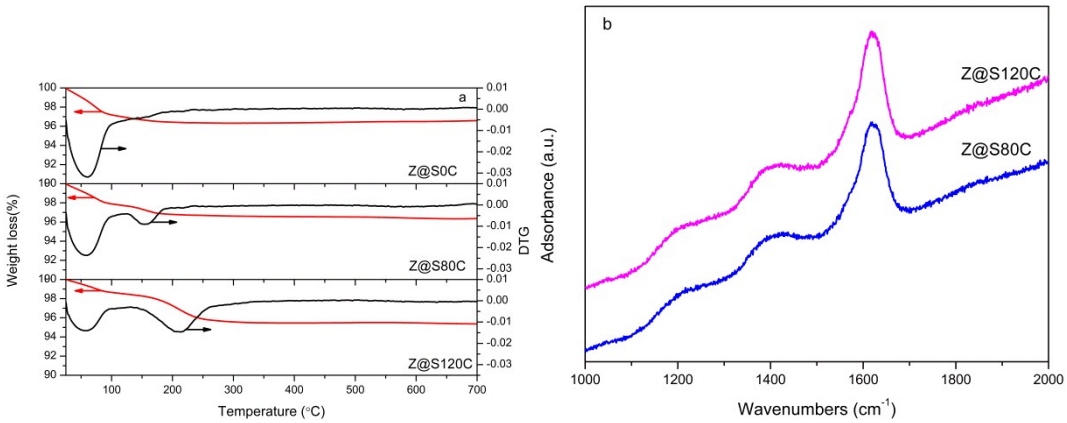

Figure S4. (a) TG and DTG profiles of Z@S0C, Z@S80C and Z@S120C, (b) UV-Raman spectra of Z@S0 and Z@S120.

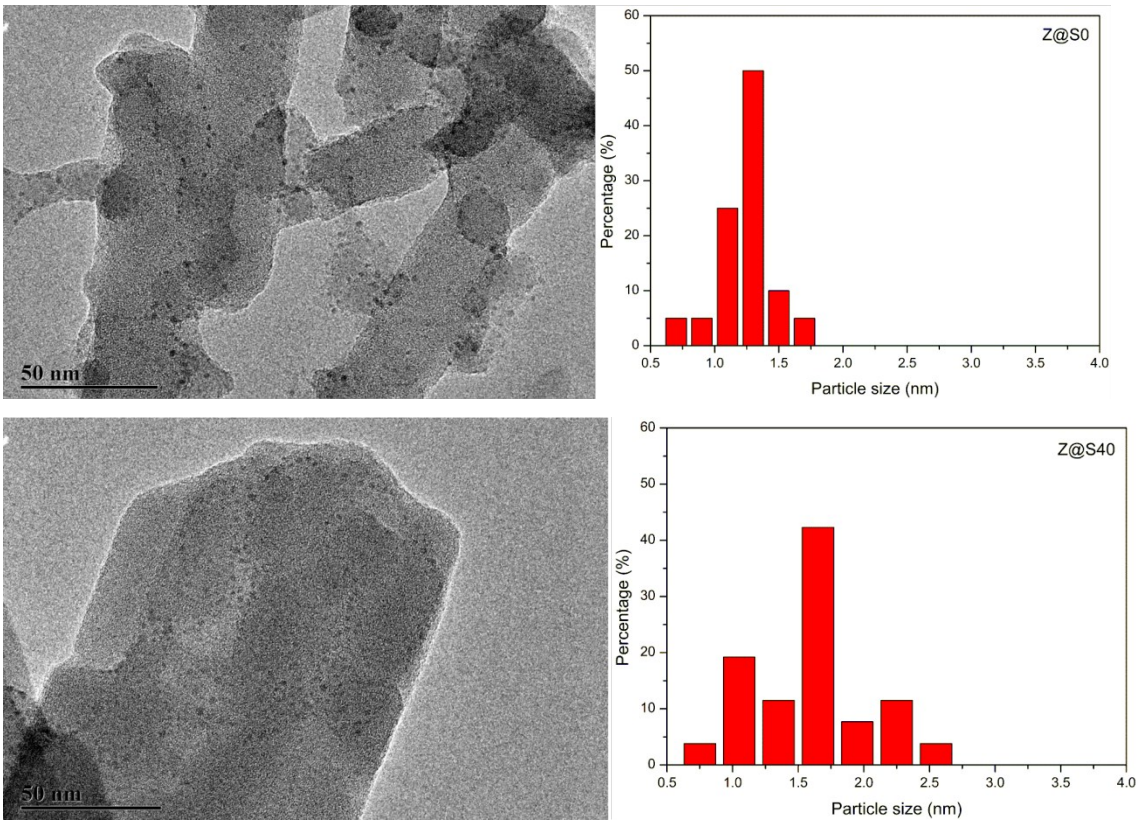

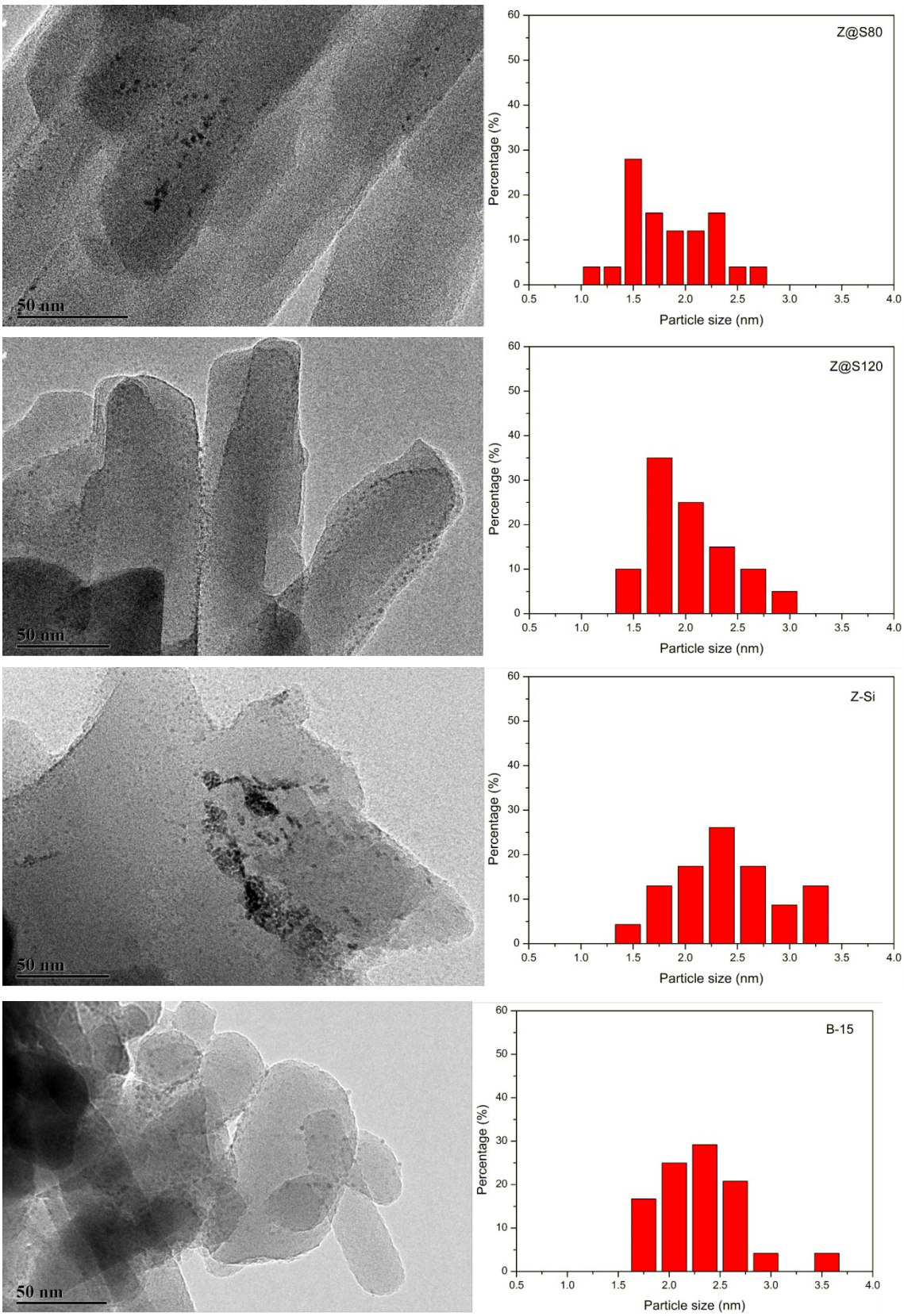

Figure S5. TEM images and particle sizes of the studied samples.

According to the widely accepted mechanism of n-alkane isomerization[1], a linear alkene is initially formed on the metal sites. Subsequently, the olefinic intermediate undergoes protonation and skeletal rearrangement on the acid sites. Finally, iso-alkene is hydrogenated on the metal sites to generate a branched alkane. Based on the bifunctional hydroisomerization mechanism, via pseudo-steady-state treatment with the assumption that olefinic intermediates isomerization was the rate-limiting step[2, 3]. The rate equation could be written as:

$$\frac{r_{isom}}{[H^+]_0} = \frac{k_{isom}K_{prot}K_{dehy}\frac{nC12}{H_2}}{1 + K_{prot}K_{dehy}\frac{nC12}{H_2}} \quad (1)$$

where K_{dehy} was the equilibrium constant for dehydrogenation of n-dodecane over Pt sites; K_{prot} were the equilibrium constant for formation of surface-bound alkoxide species by adsorption of n-dodecene on Brønsted acid sites; k_{iso} was the rate constant for isomerization of alkoxide species; $[H^+]_0$ was the number of Brønsted acid sites; [nC12] was the partial pressure of n-dodecane and $[H_2]$ was the partial pressure of hydrogen.

Eq. (1) could be written in a linear form as Eq. (2):

$$\frac{[H^+]_0}{r_{isom}} = \frac{1}{k_{isom,x}K_{prot}K_{dehy}}\frac{H_2}{nC12} + \frac{1}{k_{isom}} \quad (2)$$

The values of the apparent rate constant, k_{app}, could be obtained from the values of the slope. ($k_{app} = k_{iso}K_{prot}K_{dehy}$)[2]

Figure S6 shows the measured site-time yield of iso-dodecane as a function of n-C_{12}/H_2 molar ratio over different catalysts. Figure S7 shows reciprocal rates of iso-

dodecane as a function of H_2/n-C_{12} molar ratio. Figure S8 exhibits the Arrhenius plots for measured apparent rate constants.

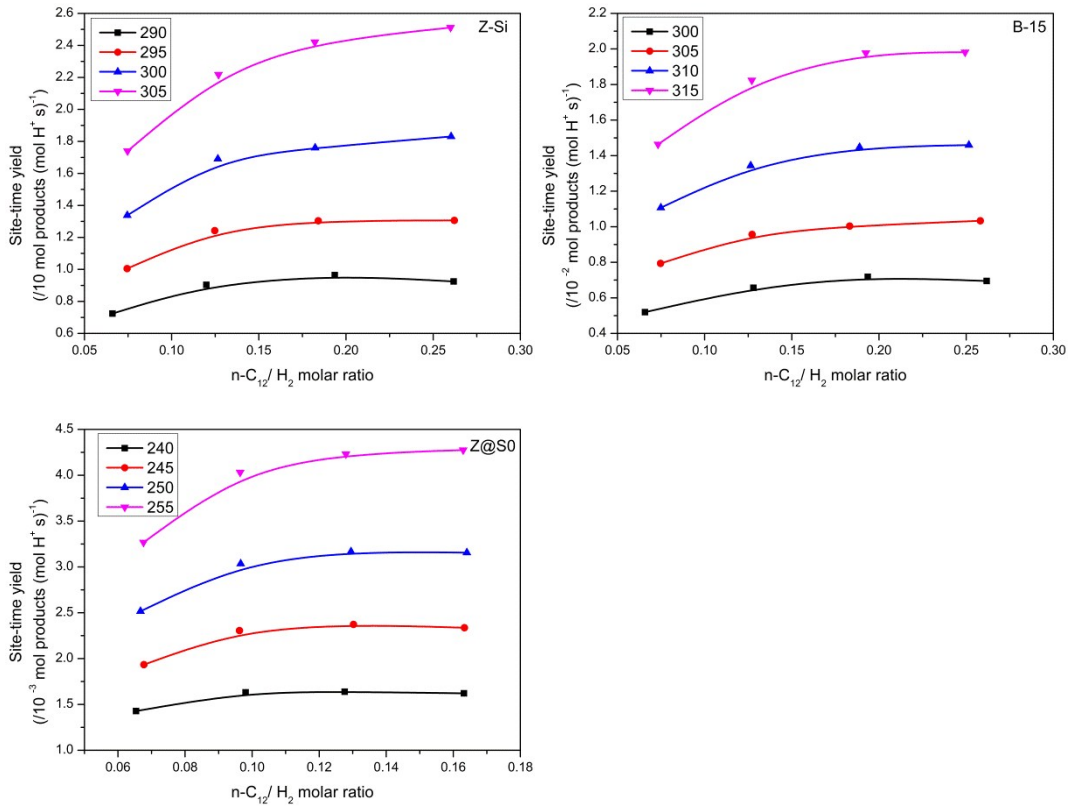

Figure S6. Measured site-time yield of iso-dodecane as a function of n-C_{12}/H_2 molar ratio over different catalysts.

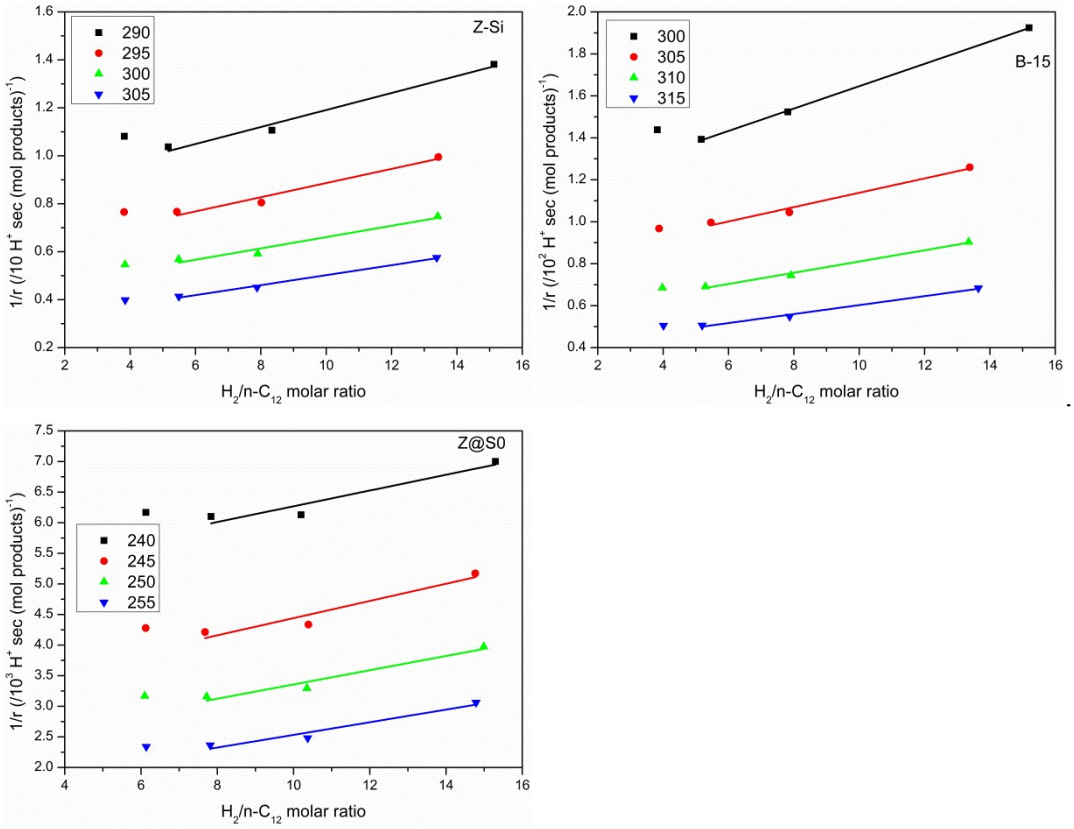

Figure S7. Reciprocal rates of iso-dodecane as a function of H_2/n-C_{12} molar ratio over different catalysts.

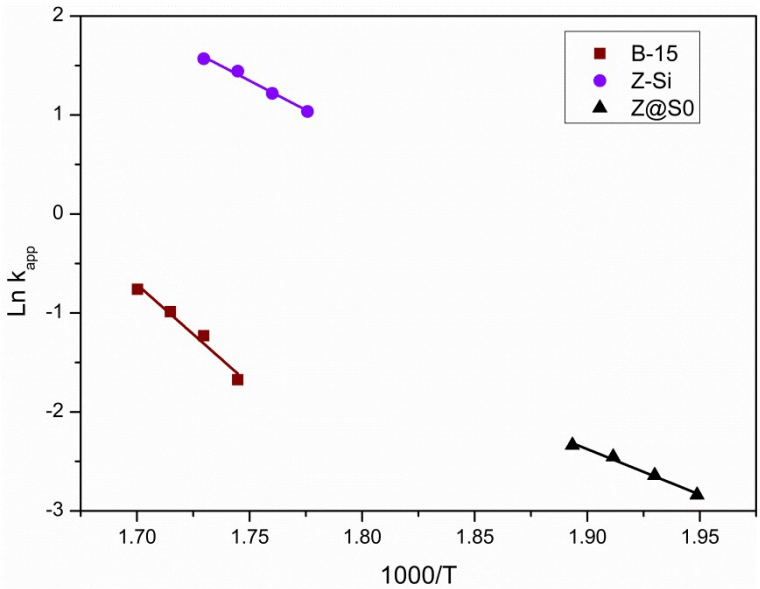

Figure S8. Arrhenius plots for measured apparent rate constants.

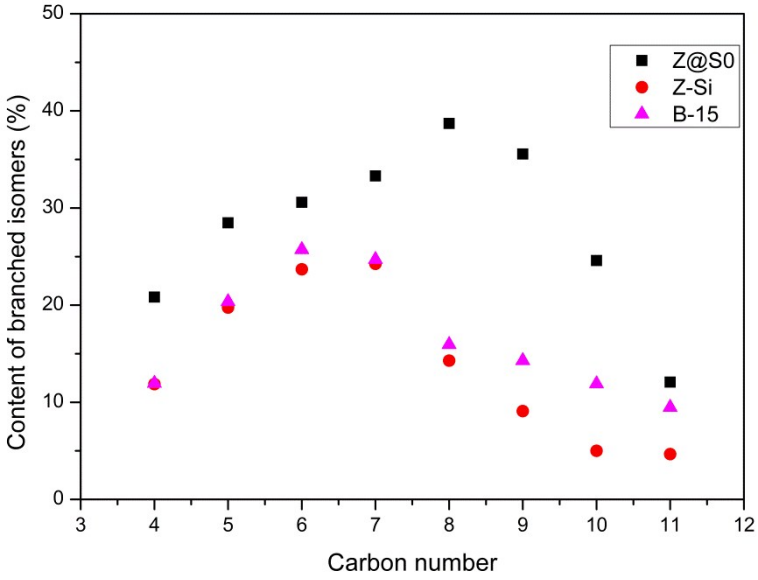

Figure S9. Content of branched products in the cracked product fractions.

Reaction conditions: H_2/n-dodecane = 750, LHSV = 1.2 h^{-1}, P = 4.0 MPa.

DFT calculation

It is well known that the catalytic activity of zeolites is mainly attributed to the acid strength of acid sites, which can be measured computationally by deprotonation energy (DPE). To compare the acidity of Al-ZSM-22, B-ZSM-22 and silanol nest-ZSM-22, DPE was used to measure acid strength due to DPE represents intrinsic acid strength of acid sites and is suitable in general cases. The calculations for DPEs were carried out with a two-layer ONIOM[4] scheme, and the quantum mechanics using B3LYP functional [5] was used as default for the QM calculations. An active inner layer, which includes a 5T cluster of the active site of zeolite, was treated using the 6-31+G(d,p) basis sets; the rest of the outer region was treated using UFF. So we denote data calculated using this method as ONIOM2(B3LYP/6-31+G(d,p):UFF), which is implement in Gaussian 09 program package.[6]

In the present work, three zeolite framework structures (Al-ZSM-22, B-ZSM-22 and silanol nest-ZSM-22) were chosen to investigate the effects of different acid sites including acidic silanol and bridging hydroxyl groups (Si-OH-Al and Si-OH-B). As shown in Figure S10, a cluster model with 72 tetrahedral sites (T-sites) was built, which consists of Al or B atom surrounded by four oxygen atoms with a hydrogen atom to balance the Brønsted acid generated at the substituted T sites. B, Al and silanol defects were placed in the T2 position, which is most stable substituted T-sites according to our previous study[7]. The deprotonation energy (E_{DP}) was calculated from Eq. (4):

$$ZOH \rightarrow ZO^- + H^+ \qquad (3)$$

$$E_{DP} = E(ZO^-) - E(H^+) \qquad (4)$$

where ZO- and ZOH represent the deprotonated and the neutral zeolites, respectively.

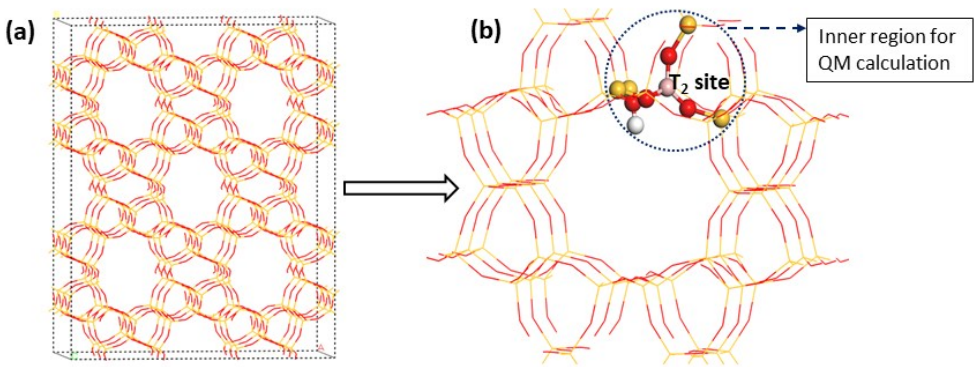

Figure S10 (a) the supercell structure of TON (ZSM-22); (b) the cluster model for QM/MM calculation: the yellow, red, white sphere stands for Si, O, H atom, respectively. The central T site can be substituted for B or Al atom. In addition, the silanol defect was built by deleting the Si atom at T_2 site.

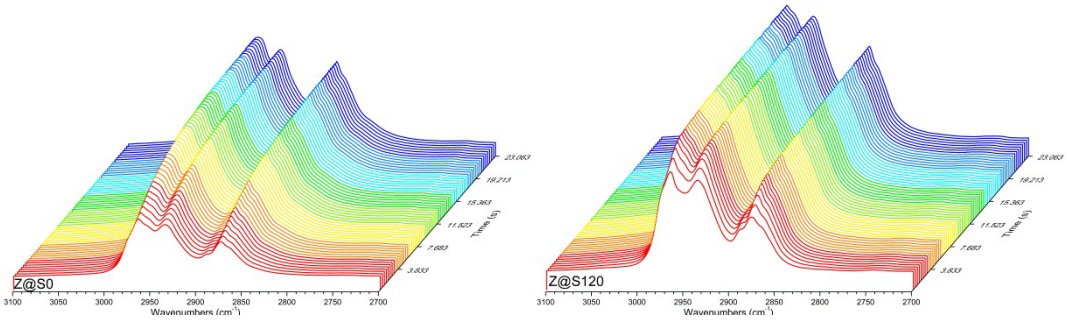

Figure S11. Changes in the IR spectra during stepwise changes in the n-hexane adsorption at 70 °C.

Table S1. Catalytic performance in n-dodecane hydroisomerization

Catalysts	Temperature °C	Conversion %	Selectivity %	Mono/Multi[a]
Z@S0	255	29.5	92.2	28.1
Z@S40	260	28.8	92	29.8
Z@S80	270	29.4	89.2	29.4
Z@S120	275	27.9	87.6	28.2
Z-Si	305	29.4	96.3	33.5
B-15	315	25.5	93.0	51.6

[a] mono-branched to multi-branched iso-dodecane ratio.

Reaction conditions: H_2/n-dodecane = 750, LHSV = 1.2 h^{-1}, P = 4.0 MPa.

REFERENCES

1. P. B. Weisz and E. W. Swegler, *Science*, 1957, **126**, 31-32.
2. H. Chiang and A. Bhan, *J. Catal.*, 2011, **283**, 98-107.
3. W. Knaeble, R. T. Carr and E. Iglesia, *J. Catal.*, 2014, **319**, 283-296.
4. F. Maseras and K. Morokuma, *J. Comput. Chem.*, 1995, **16**, 1170-1179.
5. A. D. Becke, *Journal of Chemical Physics*, 1993, **98**, 5648-5652.
6. G. W. T. M. J. Frisch, H. B. Schlegel, G. E. Scuseria, M. A. Robb, J. R. Cheeseman, G. Scalmani, V. Barone, B. Mennucci, G. A. Petersson, H. Nakatsuji, M. Caricato, X. Li, H. P. Hratchian, A. F. Izmaylov, J. Bloino, G. Zheng, J. L. Sonnenberg, M. Hada, M. Ehara, K. Toyota, R. Fukuda, J. Hasegawa, M. Ishida, T. Nakajima, Y. Honda, O. Kitao, H. Nakai, T. Vreven, J. A. Montgomery, J. E. Peralta, F. Ogliaro, M. J. Bearpark, J. Heyd, E. N. Brothers, K. N. Kudin, V. N. Staroverov, R. Kobayashi, J. Normand, K. Raghavachari, A. P. Rendell, J. C. Burant, S. S. Iyengar, J. Tomasi, M. Cossi, N. Rega, N. J. Millam, M. Klene, J. E. Knox, J. B. Cross, V. Bakken, C. Adamo, J. Jaramillo, R. Gomperts, R. E. Stratmann, O. Yazyev, A. J. Austin, R. Cammi, C. Pomelli, J. W. Ochterski, R. L. Martin, K. Morokuma, V. G. Zakrzewski, G. A. Voth, P. Salvador, J. J. Dannenberg, S. Dapprich, A. D. Daniels, Ö. Farkas, J. B. Foresman, J. V. Ortiz, J. Cioslowski and D. J. Fox,, *Gaussian 09 (Revision D.01), Gaussian Inc., Wallingford, CT*, 2009.
7. P. Y. Niu, H. J. Xi, J. Ren, M. G. Lin, Q. Wang, L. T. Jia, B. Hou and D. B. Li, *Catal. Sci. Technol.*, 2017, **7**, 5055-5068.